Spanish Journal of Palaeontology 38 (1), 23–36, 2023
https://doi.org/10.7203/sjp.26575
Sociedad Española de Paleontología ISSN 2255-0550 / eISSN 2660-9568

OPEN ACCESS RESEARCH PAPER

Dermal skeleton of the stem osteichthyan *Ligulalepis* from the Lower Devonian of New South Wales (Australia)

El esqueleto dérmico del osteíctio troncal *Ligulalepis* del Devónico Inferior de Nueva Gales del Sur (Australia)

Carole J. BURROW, Gavin C. YOUNG & Jing LU

Abstract: When first described based on isolated scales, *Ligulalepis* was assigned to the Palaeoniscoidea, a basal group of actinopterygians (ray-finned fishes). Recent cladistic analyses, mainly based on skull and neurocranial characters, have mostly recovered the taxon (or, '*Ligulalepis*') as a stem osteichthyan. Here we present information on *Ligulalepis* dermal elements other than scales and skulls, that include a skull fragment, a premaxilla, other marginal jaw elements and teeth, an accessory vomer, a partial shoulder girdle, incomplete spine-like elements, and a gular plate. The shoulder girdle and premaxilla compare closely with those of basal actinopterygians, whereas the spine-like element shows some similarity to the distal end of the spines on medial dorsal plates of the Chinese Late Silurian stem osteichthyans *Guiyu* and *Sparalepis*, or alternatively to fin rays on the stem osteichthyan *Dialipina*. One of the jaw elements appears to be a compound jugal plate plus part of the dentate maxilla, an arrangement not previously known in any Devonian stem osteichthyan, or actinopterygian. Histological structure of dermal plates somewhat resembles that of *Meemannia*, but pore openings in *Ligulalepis* lead only to the vascular canal network at the base of the ornament layer and not to a pore canal network. Like previous phylogenetic analyses, our analysis incorporating post-cranial dermal skeleton characters also recovered *Ligulalepis* as a stem osteichthyan.

Resumen: *Ligulalepis* se describió por primera vez a partir de escamas aisladas, asignándose al orden de los Palaeoniscoidea, un grupo basal de actinopterigios (peces con aletas soportadas por radios). La mayoría de análisis cladísticos recientes, basados principalmente en caracteres craneales y neurocraneales, han recuperado al taxón (*'Ligulalepis'*) como un osteíctio basal. En este trabajo presentamos nueva información sobre elementos dérmicos de *Ligulalepis* distintos de escamas y elementos craneales, que incluyen un fragmento de mejilla dentada, una premaxila, elementos mandibulares marginales y dientes, un vómer accesorio, una cintura escapular parcial, elementos tipo espinas incompletos y una placa gular. La cintura escapular y la premaxila son muy similares a las de los actinopterigios basales, mientras que las espinas muestran cierta similitud con el extremo distal de las espinas de las placas dorsales mediales de los osteíctios basales del Silúrico Superior chino *Guiyu* y *Sparalepis*, o bien con los radios de las aletas del osteíctio *Dialipina*. Uno de los elementos mandíbulares parece estar compuesto por la placa yugal y parte del maxilar, una disposición no conocida hasta ahora en ningún osteíctio del Devónico o actinopterigio. La histología de las placas dérmicas se asemeja un poco a la de *Meemannia*, pero las aberturas de los poros en *Ligulalepis* conducen solo a la red de canales vasculares en la base de la capa ornamental y no a una red de canales de poros. Al igual que los análisis filogenéticos previos, nuestro análisis, que incorpora caracteres del esqueleto dérmico postcraneal, también clasifica a *Ligulalepis* como un osteíctio troncal.

Received: 30 November 2022
Accepted: 1 May 2023
Published: 12 May 2023

Corresponding author:
Carole J. Burrow
carole.burrow@gmail.com

Keywords:
Emsian
Osteichthyes
Gleninga Formation
Troffs Formation
Taemas Formation
Palaeohistology

Palabras-clave:
Emsiense
Osteíctios
Formación Gleninga
Formación Troffs
Formación Taemas
Paleohistología

INTRODUCTION

A number of significant discoveries of early gnathostomes in recent years have contributed new data towards deciphering early osteichthyan relationships. The finds include rare cranial material from Late Silurian and Early Devonian deposits in China (*e.g.*, Zhu *et al*., 1999, 2006, 2009, 2013; Choo *et al*., 2017; Lu *et al*., 2017), as well as Canada (Schultze & Cumbaa, 2001), Siberia (Giles *et al*., 2015a) and Australia (Basden & Young, 2001; Clement *et al*., 2018). Phylogenetic analyses incorporating the new discoveries have led to revision of the taxonomic position of several taxa. For example, *Janusiscus* Giles, Friedman & Brazeau, 2015 from the Early Devonian of Siberia is now viewed as a stem gnathostome (Giles *et al*., 2015a) rather than an

actinopterygian (Schultze, 1992), and *Meemannia* Zhu, Yu, Wang, Zhao & Jia, 2006, previously considered a sarcopterygian, was proposed by Lu *et al*. (2016) to be the oldest known actinopterygian.

One taxon that has proven somewhat vexatious in these analyses is *Ligulalepis* from the Early Devonian of New South Wales, Australia. *Ligulalepis toombsi* Schultze, 1968 was erected for isolated scales from the Emsian Taemas Formation of New South Wales, and was originally described by Schultze (1968) as a palaeoniscoid. Later, Basden and Young (2001) tentatively assigned an incomplete ossified braincase and skull roof AMF101607 (first described by Basden *et al*., 2000), also from the Taemas Formation, to the same genus, with species indeterminate. Scales readily assignable to *Ligulalepis toombsi*, based on their distinctive morphology and histology, are the only palaeoniscoid type scales known from deposits of ?late Pragian–early Emsian age in south-eastern Australia, so it is reasonable to assume that dermal bones from the same deposits, with the same type of ridged ornament, should also be assigned to *Ligulalepis toombsi*. Nevertheless, recent publications have referred to AMF101607 as '*Ligulalepis*'. Based on our assessment of the disarticulated elements and the neurocrania, we consider all these specimens should be assigned to *L. toombsi*.

Speculation on the phylogenetic position of *Ligulalepis*/'*Ligulalepis*', based on features of that isolated skull, has failed to reach a consensus, with some analyses recovering it as a stem sarcopterygian (Zhu *et al*., 2009, suppl. fig. 1), a stem actinopterygian (Zhu *et al*., 2013, 2021), nested in the Actinopterygii (Long *et al*., 2015), or as a stem osteichthyan (Brazeau, 2009; Davis *et al*., 2012; Giles *et al*., 2015a; Lu *et al*., 2016, 2017; Clement *et al*., 2018). One of the recent phylogenetic analyses of early osteichthyans (Giles *et al*., 2015a, fig. 3) showed a polytomy with '*Ligulalepis*', Actinopterygii and Sarcopterygii as the sister group of *Dialipina*. Characters that were coded for '*Ligulalepis*' (and *Janusiscus*) in the analyses by Giles *et al*. (2015a) and Lu *et al*. (2016) were limited compared with most other taxa, comprising only neurocranial and skull roof features. Clement *et al*. (2018) investigated the endocranium that was first described by Basden *et al*. (2000), as well as a more recently discovered skull, using computed tomography. Like most previous phylogenetic analyses, they used only neurocranial and skull characters for '*Ligulalepis*', and their Bayesian and parsimony phylogenetic analyses recovered '*Ligulalepis*' within the stem Osteichthyes (Clement *et al*., 2018, figs. 10, 11). However, placing the taxon as the earliest diverging stem actinopterygian required only one additional step.

Other sources of information on *Ligulalepis* that could help clarify its relationships are isolated dermal bones from the Taemas Formation at Wee Jasper, as well as from ?upper Pragian–lower Emsian limestone deposits elsewhere in New South Wales (Burrow, 1994) which are attributable to the genus, and almost certainly –given the rarity of pre-Middle Devonian stem actinopterygian taxa and the lack of evidence that more than one taxon is represented– to the type species *L. toombsi*. These specimens, which we describe here, include a small fragment of a skull with some endoskeletal bone attached, a premaxilla, other marginal jaw elements and teeth, a coronoid plate, possibly an accessory vomer, a partial shoulder girdle, incomplete spine-like elements, and an incomplete gular plate.

MATERIAL AND METHODS

The holotype of *Ligulalepis toombsi* is the scale NHMUK PVP48864, from the "right bank of Murrumbidgee, boulders probably nearly *in situ*, on shore and up hillside, 2500 yds. due E. of Majurgong T. S." (Schultze, 1968, fig. 1 caption; Fig. 1A, locality 1). Most of the scales in the type material described by Schultze (1968) are from the *Spirifer yassensis* Limestone at the base of the Taemas Formation, with the majority (108 = 53.5% of all scales) from near the base level; other scales are found up into the Warroo Limestone (Fig. 1B). The incomplete skull AMF101607 assigned to *Ligulalepis* sp. by Basden and Young (2001) was collected from the vicinity of Goodradigbee Inlet at Wee Jasper, probably in the Bloomfield Limestone Member of the Taemas Formation (Fig. 1A, 1B), and another skull ANU V3628 is also from that stratigraphic level, near Rocky Flat 300 m south (Clement *et al*., 2018). The new material is from nearby localities (WJ3 and ANUV 42 sample). WJ3 is probably at the same stratigraphic level (Fig. 1A, locality 2) just above the lower *Thamnopora* zone, Bloomfield Limestone Member of the Taemas Formation (Fig. 1B) at Caravan Point and ANU V42 is from GCY loc. 24, the Massive Fish Bed type locality for *Brindabellaspis*, at the top of the Bloomfield Limestone in Goodradigbee Inlet, Wee Jasper. Other new material is from GSNSW localities C625 (skull fragment MMMC05774), C600 and C231, ?upper Pragian–lower Emsian Gleninga Formation, and C595 and C657 in the ?lower Emsian Troffs Formation, central New South Wales (Fig. 1C, 1D). Other central NSW localities were listed by Burrow (1994). One jaw fragment NHMUK PV P65806 and possible tooth whorl P65781 are from locality NHMUK 55.27, *Spirifer yassensis* Limestone.

For the phylogenetic analysis, data entry and formatting were performed in Mesquite (v.2.5); all characters were unordered and unweighted. The data matrix, comprising 278 characters and 94 taxa, was based on the analysis by Lu *et al*. (2017). Data was processed using TNT (v.1.5) software (Goloboff *et al*., 2008) for maximum-parsimony analysis using a "New technology search", with Galeaspida as the outgroup. Default settings were used for most parameters, but the value for "random additional sequence" was changed from 1 to 1000, and the Ratchet and Drift were also used during tree search. Bremer support values were generated in TNT using the script 'Bremer.run'.

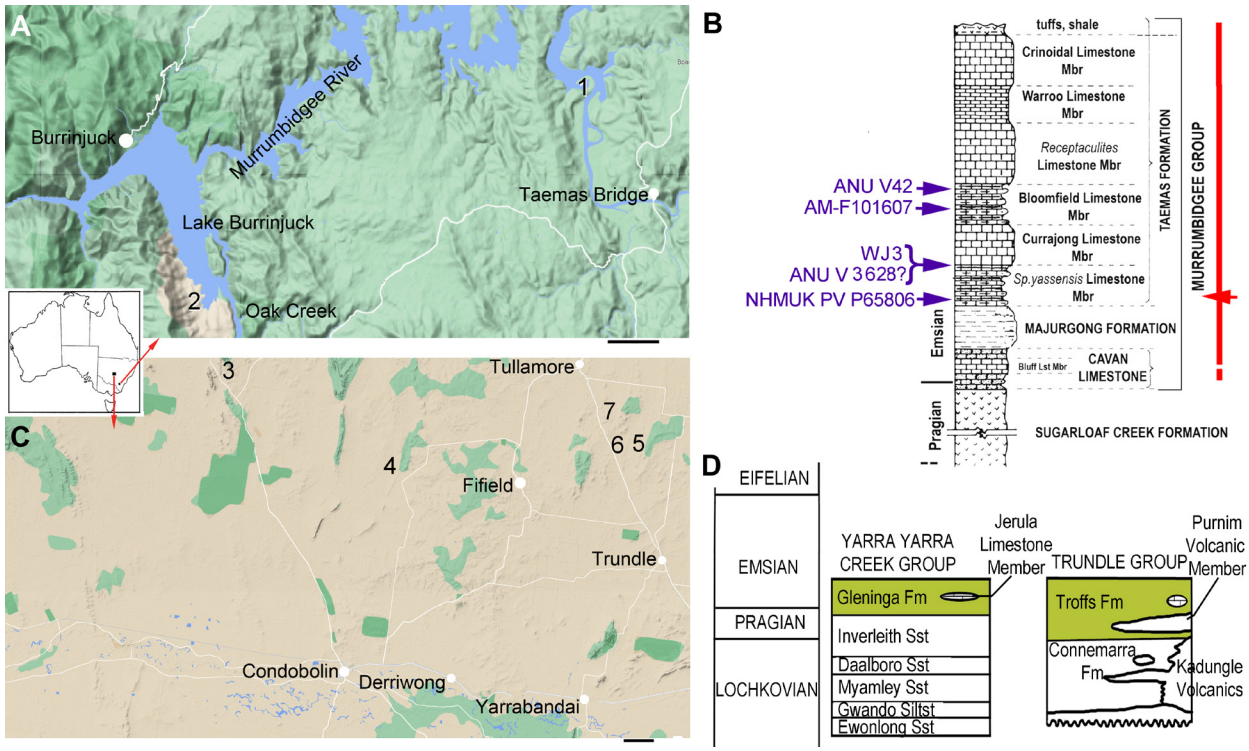

Figure 1. *Ligulalepis* occurrences in New South Wales, Australia; small inset map shows location of A and B. **A,** Google terrain map (downloaded 19-04-2023) of the Taemas-Wee Jasper region showing *Ligulalepis* localities: 1, type locality, right bank of Murrumbidgee River, and 2, Caravan Point, Wee Jasper; **B,** stratigraphic column for the Taemas Formation showing levels where *Ligulalepis* specimens have been collected (after Young, 2011, fig. 2A), specimens listed on the left are skull and jaw elements; red line on right indicates stratigraphic range where scales are found, red arrow indicates level for *Ligulalepis toombsi* holotype scale; **C,** Google terrain map (downloaded 19-04-2023) showing ?upper Pragian to lower Emsian *Ligulalepis* localities in central New South Wales: 3 = C091, 092, 231, 624, 625; 4 = C600, 608 (all Gleninga Formation: C091, 092, 624, 625, undifferentiated limestones, C231, 600, 608, Jerula Limestone Member); 5 = C287; 6 = C597; 7 = C595, 657 (Troffs Formation); **D,** stratigraphic columns for the Gleninga and Troffs formations (after Sherwin, 1996 and Jones *et al.*, 2020, fig. 1.3); *Ligulalepis* material is from the early Emsian limestones; scale bar = 2 km in A, 5 km in C.

Institutional abbreviations. **CMN,** Canadian Museum of Nature collection; **MMMC,** micropalaeontology collection of the Geological Survey of New South Wales (Natural Resources); **NHMUK PVP,** palaeontology collection of the Natural History Museum, London.

DESCRIPTION

Skull fragment MMMC05774

The dermal bone is ornamented with close-set, narrow, elongate ridges which have smooth flat crests and oblique ribbing on their sides (Fig. 2A). The anterodorsal? margin and possibly the narrow posterior margin of the bone are intact, with all other edges being fracture surfaces. Endoskeletal ossifications are fused to the inner surface of the dermal bone (Fig. 2A–2C). The only distinctive structure is an arch-shaped bone perpendicular to the dermal plate, at one end of the flat (incomplete) endoskeletal bone paralleling the dermal plate (Fig. 2B, 2C). The ornament is indistinguishable from that in Palaeozoic actinopterygians, with shiny surfaces and edge ribbing (Fig. 2E) as typifies ganoine-topped ridges.

Comparison. 3D scans of the skulls ANU V3628 and AM F101607 (Clement *et al.*, 2018, figs. 3A, 4) reveal the endoskeletal bones forming the neurocranium of *Ligulalepis*. Perhaps the canal arch on MMMC05774 could represent the excurrent nostril (cf. Clement *et al.*, 2018, fig. 3A) or the hyomandibula foramen, with the small foramen next to this being for the ramus lateralis accessorius (cf. Clement *et al.*, 2018, fig. 4B, 4C). However, the arch most closely resembles the bone surrounding the lateral cranial canal in *Raynerius splendens* (Giles *et al.*, 2015b, supp. fig. 5), indicating that the *Ligulalepis* fragment is probably the right posterolateral corner of the skull roof (Giles *et al.*, 2015b, suppl. fig. 3f, showing the left posterolateral corner in *Raynerius*). A lateral cranial canal is considered to be a key actinopterygian feature (Lu *et al.*, 2016, fig. 4).

Jaw element MMMC05784, a composite element comprising maxilla and jugal?

This element from Wee Jasper locality WJ3 is an L-shaped bone with a smooth concave inner margin that is presumed to be circumorbital. The anterior margin has an overlap surface, the posterior margin is slightly convex, and the ventral (occlusal) margin has a

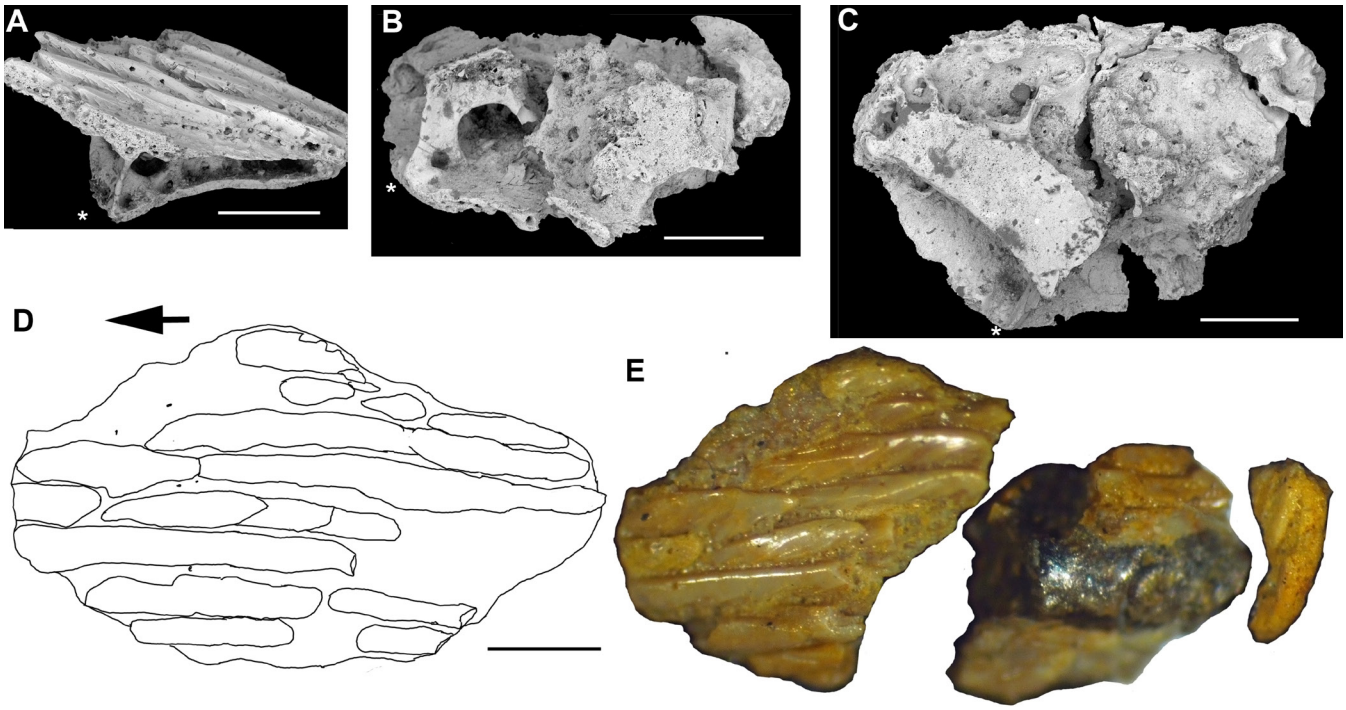

Figure 2. Cranial fragment MMMC05774 from locality C625. **A–C,** SEM images; **A,** lateral view; **B,** internal-lateral view; **C,** internal view; **D,** sketch of external view, before fracture; **E,** external view after fracture, light microscope image; scale bar = 0.5 mm, anterior to left, asterisk indicates the same point on A–C.

row of tooth sockets along its length, possibly with some smaller sockets lateral to this row, and two ankylosed teeth preserved near the posterior corner. Ornament comprises short ganoine-covered dentine ridges near the tooth row; ridges become more elongate dorsally on the plate. A row of pores for the suborbital sensory line canal are aligned paralleling the circumorbital margin on the external surface, and the internal surface is pierced by large pores approximately midway between the tooth row and the circumorbital edge, and towards the posterior margin higher up.

Comparison. The shape of this bone most closely resembles the jugal in Carboniferous coelacanth *Hadronector donbairdi* Lund & Lund, 1985, but that bone (like all jugals in coelacanths) lacks teeth. A combination jugal-maxilla is a feature of the Recent *Polypterus bichir* (*e.g.*, Gardiner, 1984, fig. 77B), but all Devonian actinopterygians have a separate jugal forming the posteroventral margin of the orbit above the tooth-bearing maxilla. The combination of an occlusal tooth row plus a sensory line on MMMC05784 indicates that this element represents a jugal + maxillary bone. The overlap surface on the anterior end of the bone shows that the upper jaw had more than one tooth-bearing bone behind the premaxilla. Articulated specimens of *Dialipina salgueiroensis* Schultze, 1968 that preserve the head region appear to show a long narrow maxillary plate as described by Schultze and Cumbaa (2001), but perhaps it actually comprises two plates, one anterior and another posterior to the orbit, as there appears to be a short break visible in the figured specimen CNM 51125 (Schultze & Cumbaa, 2001, fig. 18.1).

Other tooth-bearing jaw elements and a possible parasymphysial tooth whorl from Taemas-Wee Jasper

ANU V42b (Fig. 3G–3I) is a 7.5 mm long fragment of a dentary; the posterior and anterior ends have broken off. Three of the main teeth are preserved, with at least one of these teeth appearing to have a tip that is shinier than the base of the tooth. The outer surface of the element is covered with contiguous, shiny, short and long ridges comparable to the dermal bone ornament on the '*Ligulalepis*' skulls illustrated by Clement *et al.* (2018, figs. 2, 4).

ANU V42a (Fig. 3J–3K) is a 3.9 mm long posterior end of a dentary (see the dentary of *Mimipiscis* in Gardiner, 1984, fig. 92 for comparison), with one intact marginal tooth and bases of three other teeth preserved, all separated by round pits of the same diameter as the tooth bases. The medial surface towards the posterior end is depressed, presumably to overlap the articular. A row of pores on the medial surface, running back from the middle of the anterior fracture surface then down below the third preserved tooth towards the lower edge of the element, are presumed to open into a mandibular canal. The outer surface bears ornament comparable with that on other *Ligulalepis* dermal bones.

NHMUK PV P65806 (Fig. 3L; Basden, 2001, figs. 4–19M) is a coronoid with one large tusk plus three small teeth, and a narrow labial field of small denticles. A large foramen opens in the centre of the element between the large cusp and one of the smaller teeth. The plate is very thin with a strongly concave base.

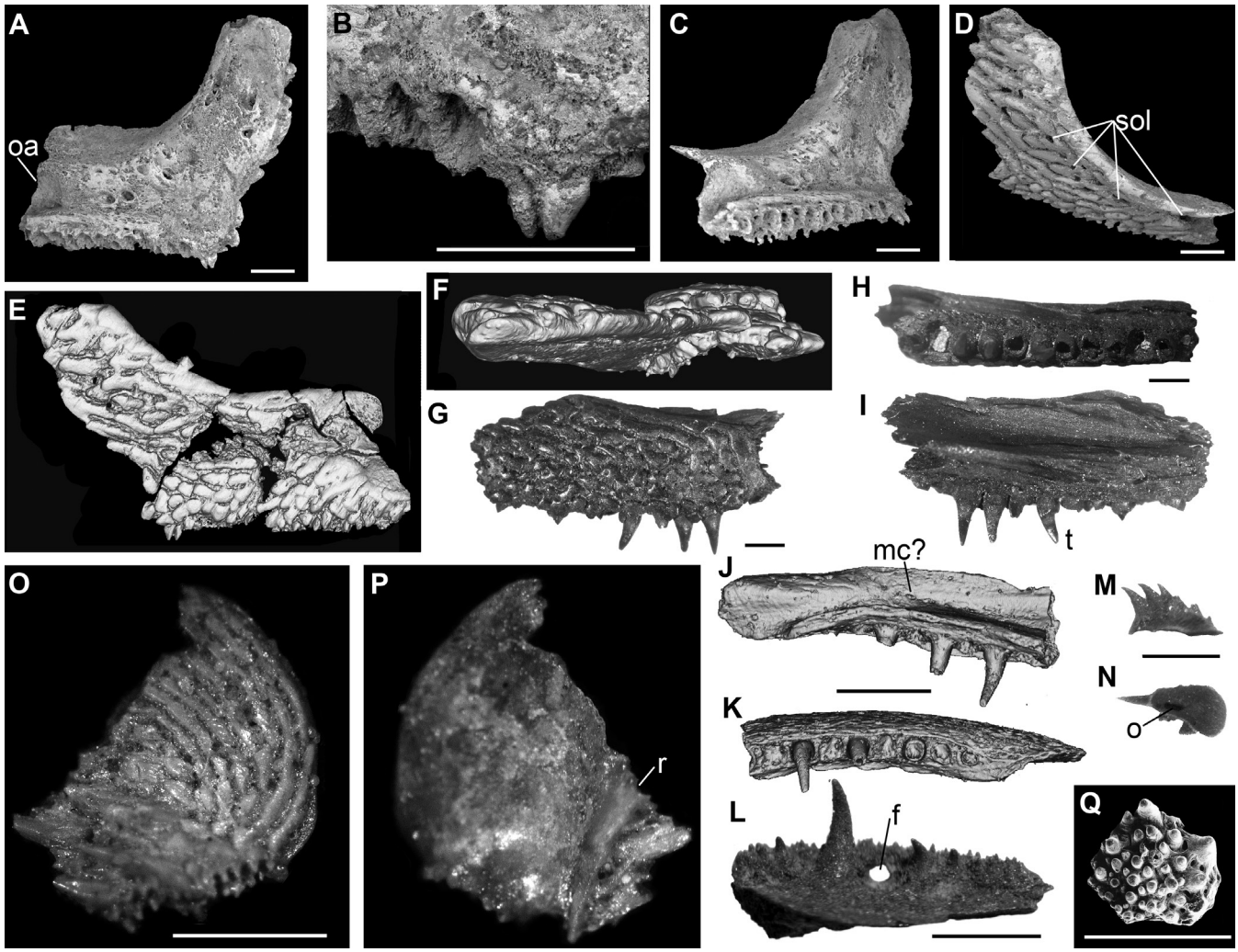

Figure 3. Jaw and dentition elements of *Ligulalepis toombsi* (A–N from Taemas-Wee Jasper, O–Q from central NSW). **A–G,** Left maxilla+jugal? MMMC05784 from locality WJ3; **A,** medial view; **B,** medial view of teeth preserved at posterior end of element; **C,** occlusomedial view; **D,** dorsolateral view; **E–F,** 3D scan images after damage to specimen, lateral, dorsal and occlusal views (to same scale as D); **G–I,** Burrinjuck dentary fragment ANU V42b in lateral, occlual and medial views; **J–K,** 3D scan images of ANU V42a dentary fragment in medial and occlusal views; **L,** first coronoid NHMUK PV P65806, medial view; **M–N,** possible parasymphysial tooth whorl NHM UK PVP65781 in lateral and basal views; **O–P,** right premaxilla MMMC05775 from C600 in external and internal views; **Q,** ?possible accessory vomerine toothplate MMMC05776 from C657 in crown view. **f,** foramen; **mc,** mandibular canal pores; **o,** opening in base; **oa,** overlap area; **r,** ridge; **sol,** suborbital sensory line pores; **t,** tooth; **tt,** shiny tooth tip; scale bars = 1 mm.

Given the lack of a medial lamina and the size of the teeth, by comparison with the coronoids of *Mimipiscis* (Gardiner, 1984, fig. 90) this is probably a first coronoid. NHMUK PV P65781 (Fig. 3M, 3N) is an asymmetric tooth or denticle whorl with a medial row of six single-cusped teeth that increase in size towards the narrower end of the base, the mesial surface of which is concave laterally and anteroposteriorly. A pulp cavity opens out medially through the base beneath the second-largest tooth (Fig. 3N). The whorl differs from those of 'acanthodians' in having only a very thin basal plate, and bears a resemblance to the dentary tooth whorl of *Howqualepis* (Long, 1988, fig. 21) in having six monocuspid teeth. However, the only known example of the *Howqualepis* element is preserved as an impression, medial to the anterior end of the left dentary and its structure and type of attachment is unknown. NHMUK PV P65781 is only tentatively assigned to *Ligulalepis*, given its small size (*ca.* one-tenth that of the *Howqualepis* whorl) and lack of closely comparative elements in other stem osteichthyans.

Toothed dental elements from central NSW

MMMC05775 (Fig. 3O–3P) from GSNSW locality C600 is probably an incomplete right premaxilla. As preserved, it is a semicircular element with two rows of small denticles along part of the circumference, with a broken edge along the 'diameter'. The external ornament comprises elongate narrow ridges paralleling the circumference over most of the surface, plus shorter spinelet-like ridges extending laterally from the denticulated edge. The flat ridges bear the distinctive oblique

microridges along the sides that characterise the shiny outer enameloid layer in many Devonian actinopterygians (*e.g.*, *Cheirolepis canadensis* Arratia & Cloutier, 1996, fig. 13C; *Moythomasia lineata* Choo, 2015, fig. 4C; *Pickeringius acanthophorus* Choo *et al*., 2019, fig. 8J). The internal surface is relatively smooth except for a sharp curving ridge running dorsoventrally (Fig. 3P). By comparison with premaxillae on articulated actinopterygians (*e.g.*, from the Frasnian Gogo Formation of Western Australia: *Mimipiscis*, see Choo, 2011, fig. 11G, and *Gogosardinia*, see Choo *et al*., 2009, fig. 8a-8d), the fracture probably runs along the line of a sensory canal. Unlike the premaxillae of these Gogo fish, the preserved part of the Troffs Formation element lacks larger teeth along the occlusal margin.

MMMC05776 from GSNSW C657 (Fig. 3Q) is possibly an accessory vomerine toothplate of *Ligulalepis*. The polygonal toothplate is *ca.* 1.0 mm wide and bears two large, and *ca.* 30 medium and small, upright smooth teeth clustered over the plate. The large teeth abut one edge. The flat base is vacuous, with wide openings around the bases of the teeth. A broken central tooth shows a wide central pulp canal. The large teeth appear to have a denser tissue forming the tip.

The plate resembles the accessory vomers of *Moythomasia durgaringa* Gardiner & Bartram, 1977 from the Frasnian Gogo Formation, which have a similar layout with two or three large teeth along the posterior edge in a field of small teeth (Gardiner, 1984, fig. 51).

Tooth histology

Jaw fragment MMMC04754 (Fig. 4A–4B) from the GSNSW locality C657 was a short segment, lacking external ornament, and originally bearing six or seven rounded teeth. The anterior? end with the largest tooth was broken off to make a vertical coronal section MMMC04755 (Fig. 4C–4D; Schultze, 2016, fig. 13). Clement *et al*. (2018) suggested this jaw fragment could be from a different taxon, however an onychodont is the only other osteichthyan known from this locality, and the teeth lack a socketed base as characterises onychodont teeth; as far as known, none of the non-osteichthyans ('placoderms', acanthodians) from the locality have orthodentine in their teeth. The tooth is formed of a clear tissue with unbranching dentine tubules, which Schultze (2016) interpreted as acrodin, extending out towards the tooth surface. A few dentine tubules extend up from the pulp cavity in the base of the tooth. The height of the clear dentinous area corresponds to the height of the tooth above the bone base in the original specimen, suggesting that the unbranching tubules are the orthodentine of the pallial tooth tissue, and the tubules rising up from the pulp cavity are circumpulpal tissue, surrounded by bone. Another small jaw fragment MMMC05779 from GSNSW locality C231 had three higher, conical teeth, in which the tip appears on superficial examination to be a different tissue to the rest of the tooth (Fig. 4E–4F). This different appearance is probably caused by hyphal borings in the tip, based on MMMC05780, a vertical sagittal section of the middle tooth (Fig. 4G–4H). This section shows the primary (pallial) tooth tissue contains unbranching dentine tubules; this tissue extends down the sides as well as on top of the secondary (circumpulpal) dentinal tissue, with no clear demarcation between the outer and inner dentine layers. The teeth appear to have a very thin outer birefringent layer on one side (Fig. 4D), but it is unclear if the dentine tubules extend into this layer.

An acrodin cap on teeth is one of the 10 'key features' for the Actinopterygii recognized by Lu *et al*. (2016).

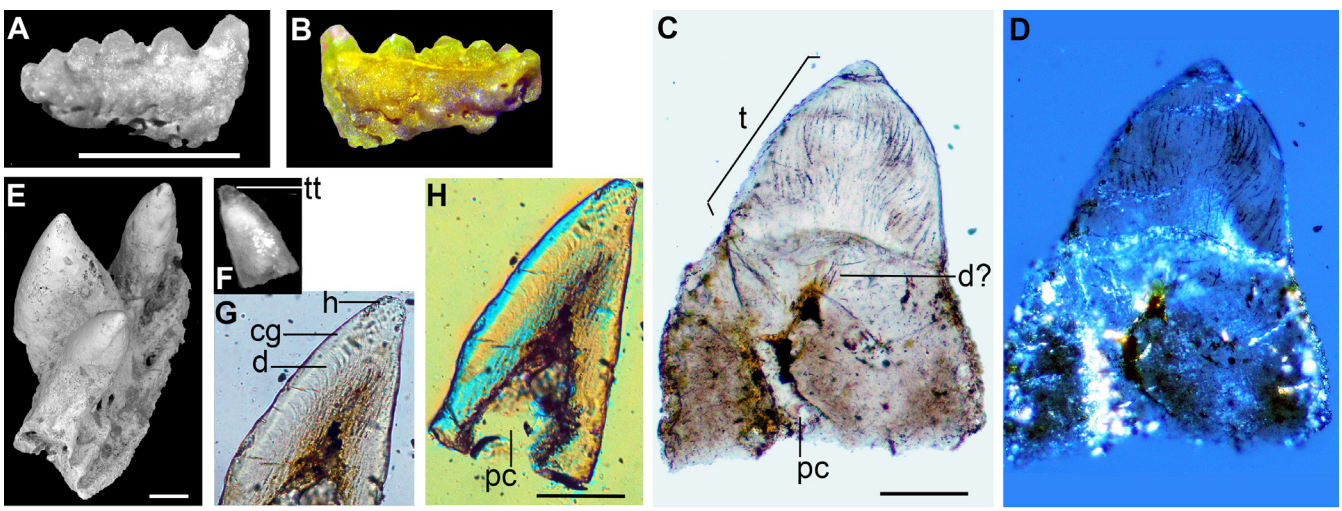

Figure 4. Isolated teeth of *Ligulalepis toombsi* from the Troffs and Gleninga formations, morphology and histology. **A**–**B,** Jaw fragment MMMC04754 with five teeth in lingual and labial views, greyscale and colour light microscope images; **C**–**D,** vertical section MMMC04755 of the tooth at right in (A); **C,** unpolarised; **D,** Nomarski optics; **E**–**G,** jaw fragment MMMC05779 from C231 with three ankylosed teeth (broke up during ESEM); **E,** SEM of fragment before breakage; **F,** middle tooth of the jaw fragment, light microscope image; **G,** vertical section MMMC05780 of the tooth in (F); **cg,** collar ganoine; **d,** orthodentine; **h,** hyphal borings; **pc,** pulp cavity; **t,** differentiated tooth tip; scale bars = 1 mm in A–B, 0.1 mm in C–H.

Teeth with a superficial enameloid layer are found in some stem osteichthyans. Zhu *et al*. (2009, suppl. 2, fig. 9c–9e) noted that *Guiyu oneiros*, a taxon that is perhaps the most basal stem sarcopterygian, has teeth with an enameloid outer layer but lacking an acrodin cap. *Meemannia eos*, recovered by Lu *et al*. (2016) as the most basal actinopterygian, also lacks an acrodin cap and it is unknown whether its teeth have enameloid or not. It is only in actinopterygians more derived than *Cheirolepis* that an acrodin cap is generally considered to be present. However, the histological structure of teeth in very few Devonian actinopterygians is known, with identification of acrodin sometimes based on superficial appearance (*i.e.*, the tip is shinier than the rest of the tooth) rather than histology (*e.g.*, Giles *et al*., 2015b, suppl. fig. 6d). The identification of an acrodin cap in tooth thin section MMMC04755 by Schultze (2016) was an interesting –and apparently controversial– observation. Based on the thin sections MMMC04755 and MMMC05780 which are both assigned here to *L. toombsi*, we now think that acrodin is not present, and the tissue previously identified as such in the teeth is orthodentine.

Dermal pectoral girdle MMMC05781 (incomplete cleithrum, possibly with postcleithrum)

This distinctive, probably compound element (broken into four pieces) from GSNSW locality C595 has a maximum length of 3 mm along the dorsal margin, and a maximum height of 4.5 mm as preserved. The ornament comprises shiny flat petal-like tubercles with subparallel ridges (Fig. 5A, 5B, 5E). Pores open out through and between the tubercles. An overlap area extends along the outer surface of the ventral edge, presumed to be where it was overlapped by the clavicle. The anterior margin is smooth and concave (Fig. 5A, 5C–5E). The dorsal margin has broken off anteriorly; the posterior margin is preserved on the upper fragment (Fig. 5F), but has broken off the lower posterior fragment (Fig. 5G). Bone is thickest along the

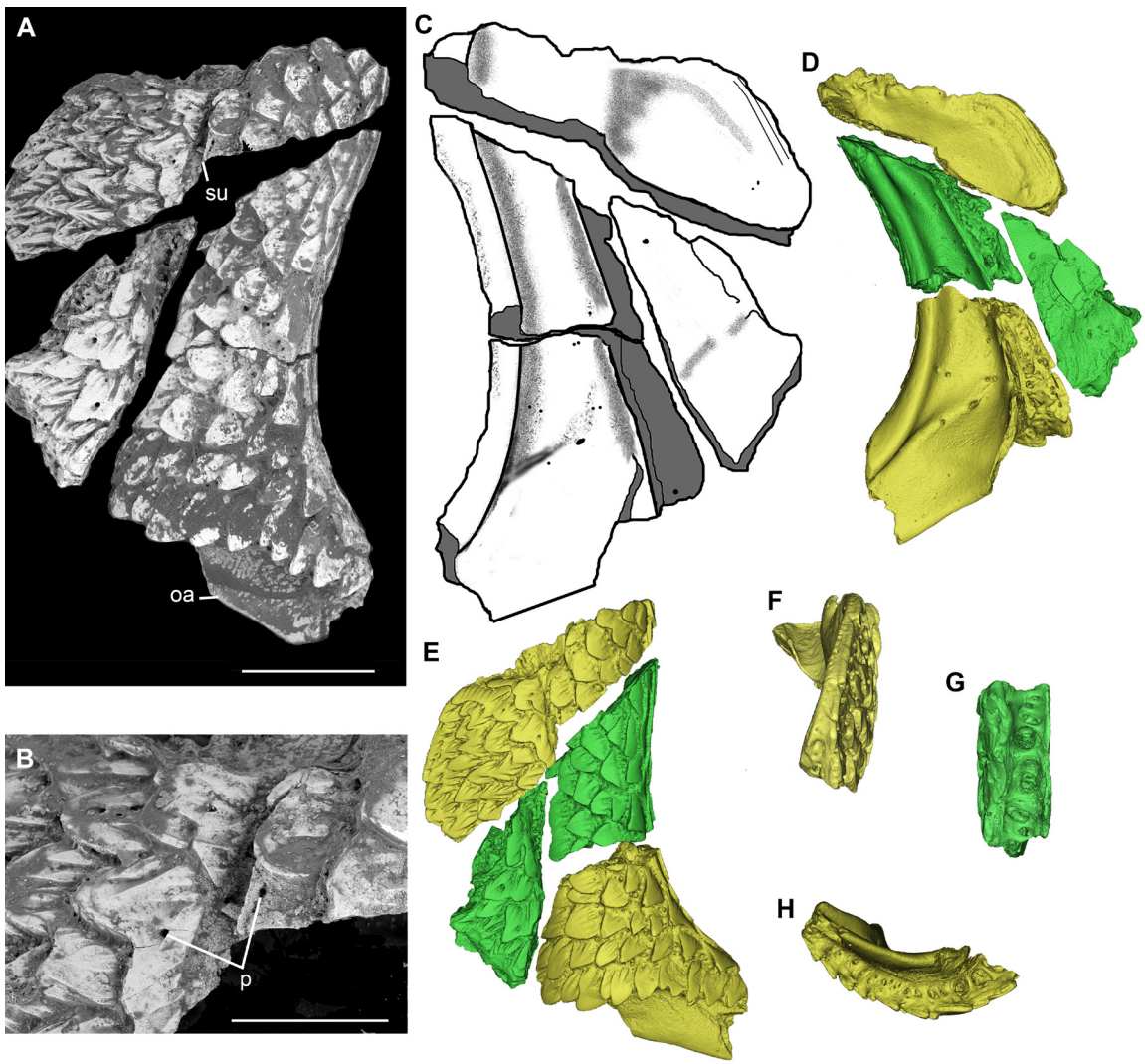

Figure 5. Dermal shoulder girdle MMMC05781 of *Ligulalepis toombsi* from locality C595, Troffs Formation. **A**–**B,** ESEM images of lateral view of fragments; **C,** sketch of medial view; **D**–**H,** 3D scan images, **D,** medial view; **E,** lateral view; **F,** posterior view of upper fragment; **G,** posterior view of anterior middle fragment; **H,** ventral view of lower fragment; **oa,** overlap area; **p,** pore; **su,** ?suture line; scale bars = 1 mm in A, 0.5 mm in B.

anterior edge, with a rounded ridge running along this margin on the internal surface (Fig. 5C, 5D). Behind the ridge, the surface is smooth and pierced by several foramina aligned parallel to the vertical fracture edge (Fig. 5D). A lower ridge extends posterodorsally from the ventral end of the anterior edge. Ornament on the upper fragment has a narrow vertical gap near its centre, aligned with a slight swelling on the internal surface, possibly marking a suture line.

Comparison. The general shape of the cleithrum corresponds to that of Devonian actinopterygians including *Cheirolepis*, *Moythomasia*, and *Mimipiscis*. As the posterior edge is not preserved, it is not known if the element had a posterior embayment for the pectoral fin, as seen on these other taxa, but based on the shape and ornament it appears unlikely to have had a spinal process like that of stem sarcopterygians *Psarolepis* Yu, 1998, *Guiyu* Zhu, Zhao, Jia, Lu, Qiao, & Qu, 2009, and *Sparalepis* Choo, Zhu, Qu, Yu, Jia, & Zhao, 2017. Friedman and Brazeau (2010, fig. 6) modified Schultze and Cumbaa's (2001) interpretation of the dermal shoulder girdle in *Dialipina*, identifying a

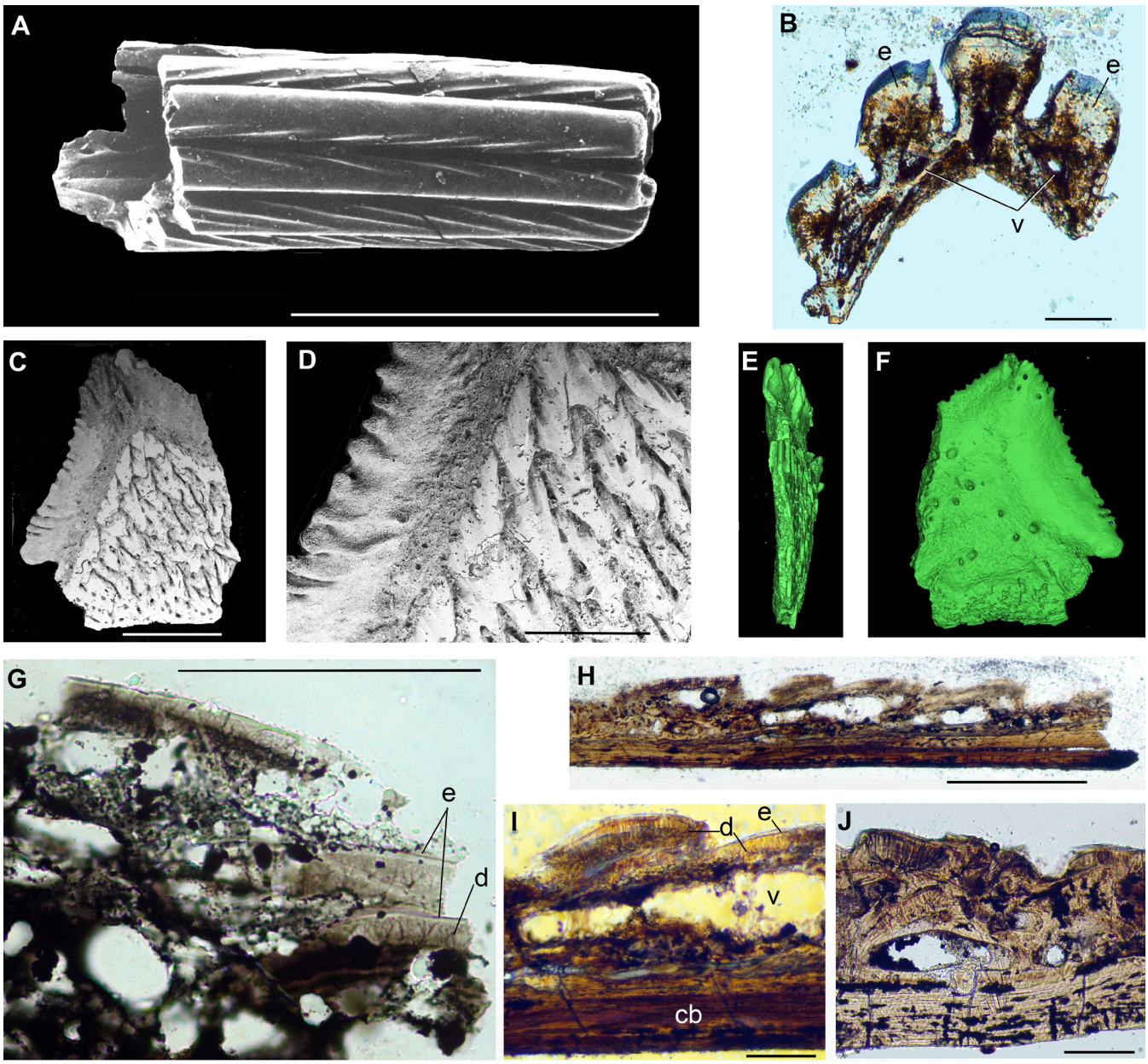

Figure 6. Other dermal bones of *Ligulalepis toombsi*. **A**–**B,** Spine fragments from locality C657, Troffs Formation; **A,** SEM image of spine fragment MMMC05777; **B,** thick partial transverse section MMMC05778 of spine fragment (thickness of the section shows as the blue above the thin enamel layer); **C**–**F,** dermal plate, incomplete ?lateral gular MMMC05785 from Caravan Point locality; **C**–**D,** SEM images of external surface; **E**–**F,** 3D scan images showing edge and internal views; **G,** vertical longitudinal thin section MMMC05786 of plate fragment, riddled with fungal or algal borings; **H**–**J,** vertical thin sections of dermal bone from C595, Troffs Formation; **H**–**I,** vertical longitudinal section MMMC05782; **J,** vertical transverse section MMMC05783; **cb,** cellular bone base; **d,** dentine; **e,** enamel; **v,** vascular canal or space; scale bars = 1 mm in A, C, 0.5 mm in D, 0.1 mm in B, G–J.

supracleithrum, postcleithrum and cleithrum. It seems probable that the vertical ornament gap on the upper *Ligulalepis* fragment is along a suture line between the cleithrum and postcleithrum, with the latter being complete. However, the basal bone layer is continuous under both elements, with no evidence of separation between them. Anteriorly, the ornament appears continuous between the upper and lower fragments, indicating that they are both parts of the cleithrum rather than being the cleithrum plus a supracleithrum. In *Dialipina* the postcleithrum is large relative to that in more advanced osteichthyans (Friedman & Brazeau, 2010, fig. 6B); if correctly interpreted, the *Ligulalepis* postcleithrum is also relatively large, with both these taxa thus differing from younger, actinopterygian taxa which had only a small, scale-like postcleithrum, if they had one at all (Gardiner, 1984, p. 374). Presence of a clavicle is inferred from the clearly demarked overlap area anteroventrally on the cleithrum. Ornament on this dermal complex is comparable with that on dermal shoulder girdles of stem osteichthyan *Andreolepis hedei* (Janvier, 1978, pl. 1) and actinopterygian *Cheirolepis trailli* Agassiz, 1835 (Pearson & Westoll, 1979, fig. 12a–12c) where the ornament also comprises short ridges and flat tubercles. The posterodorsally directed ridge on the internal surface probably represents an attachment area for the scapulocoracoid.

Spine-like elements

The incomplete but distinctive structure MMMC05777 from GSNSW C657 has a circular cross-section and is ornamented with closeset enamel?-covered longitudinal ridges with oblique microridges along their sides (Fig. 6A), identical to the ridges on the skull fragment (Fig. 2). A transverse thin section MMMC05778 of an end of a fragment of a similar element (Fig. 6B) shows a thin compact inner layer around the central cavity, a large calibre longitudinal canal underlying each ridge with fine dentine tubules radiating out towards the external surface of the ridge. A single thin outer enamel? layer is barely distinguishable.

Slender ornamented spines are not known from any stem osteichthyans. *Lophosteus* Pander, 1856 has robust spines with an open pulp cavity (Gross, 1969, fig. 3D–3J; Jerve *et al*., 2016, figs. 6–13), resembling the prepectoral and prepelvic spines of climatiid acanthodians in having inclined ribbed tubercles (*e.g.*, Burrow *et al*., 2015, fig. 2A, 2H). The spines we assign to *Ligulalepis* also differ from the spines of diplacanthid and ischnacanthiform acanthodians: those spines have smooth longitudinal ridges, but have a median sulcus along the trailing edge of the spines and lack the oblique microridges (*e.g.*, Burrow *et al*., 2016, 2018). *Psarolepis*, *Guiyu*, and *Sparalepis* have robust dorsal and pectoral spines extending from basal plates. In *Psarolepis* the spine surface is a shiny enamel pierced by rows of large pores (Zhu & Schultze, 1997, fig. 3) as typical of cosmine, whereas in *Guiyu* (Zhu *et al*., 2009, fig. 2c, 2d) and *Sparalepis* (Choo *et al*., 2017, fig. 3C) the dorsal spines appear to have smooth longitudinal ridges. At least one specimen of *Dialipina salgueiroensis* Schultze, 1968, a taxon recovered in most recent analyses as the most basal osteichthyan, appears to have multiple elongate rays or spines in an indeterminate position (CMN And8-3-29; Fig. 7A–7B). Perhaps the spine like element from *Ligulalepis* could be a structure comparable to those elements, although the *Dialipina* spines have been fractured lengthwise and few details, other than their unjointed structure, can be distinguished. Zylberberg *et al*. (2015) examined the histological structure of scales, fulcra and lepidotrichia in *Cheirolepis canadensis* (Whiteaves, 1881), showing that even the unsegmented basal ends of the lepidotrichia are formed of two hemisegments, and fulcra are essentially elongate scales; both differ from the cylindrical structure of MMMC05777. Burrow (1994, figs. 4n, 4o, 5g) showed that *Ligulalepis* had relatively 'normal' (cf. actinopterygian) elongate, interlocking lepidotrichia. We can only conclude that *Ligulalepis* had spine like elements, but their position on the body is unknown.

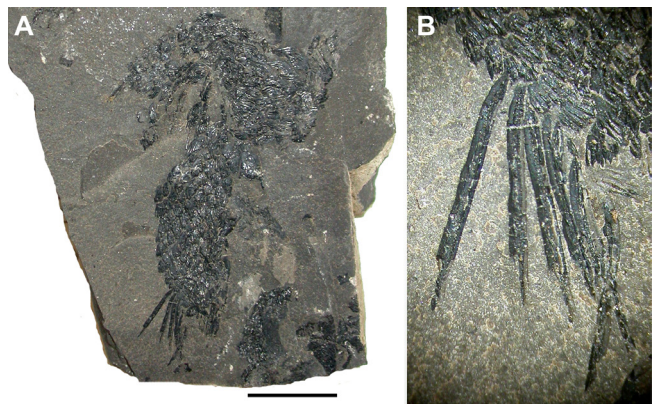

Figure 7. *Dialipina salgueiroensis* CMN And8-3-29 from the Lower Devonian Bear Rock Formation; Anderson River, western Canadian Arctic. **A,** Whole specimen; **B,** closeup of spine-like elements; scale bar = 10 mm in A.

Gular plate MMMC05785 from Wee Jasper

This incomplete, rhombic dermal plate from Wee Jasper locality WJ3 has wide unornamented overlaps with a 'frilled' margin along the two anterior edges (orientation inferred from the ornament layout), and ornament comprising elongate flat, overlapping tubercles/short ridges oriented parallel to the presumed long axis of the element (Fig. 6C–6E). It appears to have been a slightly asymmetric element when complete. The frilled margin is more elaborately developed along the left edge (Fig. 6C), and there is a curving ridge parallel to this edge on the internal surface (Fig. 6F). Pores open out on and between the tubercles (Fig. 6D); the inner surface is smooth with scattered canal openings (Fig. 6F).

Comparison. Unpaired median gular plates have a rhombic shape similar to that presumed to be the original shape of this element, however they are more or

less symmetric. Also, median gulars usually lack, or have a minimal, unornamented margin (*e.g.*, Frasnian actinopterygians *Mimipiscis toombsi* and *Moythomasia durgaringa* (Gardiner, 1984, figs. 97, 100, respectively) and *Raynerius splendens* (Giles *et al*., 2015b, fig. 1)). Of other possible identifications, lateral gular plates are also asymmetric, subrhombic, with ornament oriented along the long axis. Although in some taxa the plates lack or only have minimal unornamented edges (*e.g.*, *M. durgaringa* Gardiner, 1984, fig. 100), other taxa have wide overlap areas on the anterior part of the plate (*e.g.*, *Wendyichthys dicksoni* and *Cyracorhis bergeraci* Lund & Poplin, 1997, figs. 4, 16B). The interclavicles of *Mimipiscis* and *Moythomasia* are elongate with a pleated margin along the two posterior edges (Gardiner, 1984, figs. 130, 134), the opposite arrangement to that in the Wee Jasper plate, and they have only a small central ornamented area surrounded by expansive smooth areas. It seems most likely that MMMC05785 is a lateral gular plate.

Histological structure of dermal plates

A fragment of plate MMMC05786 from Wee Jasper was sectioned vertically through the long axis of ornament ridges to show the histological structure (Fig. 6G), confirming that the ornament has single layered enamel covering each tubercle or ridge. Pores that penetrate the ornament ridges, or open out between the ridges and tubercles, connect to the vacuous canal network in the spongiose layer between the ornament and the basal bone layer. As in the spine, each ridge has a longitudinal canal near the base from which the fine dentine tubules radiate towards the outer surface. Dermal bone fragments from GSNSW C595 were also sectioned vertically along the ridges (Fig. 6H–6I) and transversely across the ridges (Fig. 6J). These sections MMMC05782 and MMMC05783 show the same composition, but their better preservation shows the lamellar cellular bone forming the basal layer, as also originally identified by Schultze (1968, fig. 5) in *L. toombsi* scales. Schultze *et al*. (2021, p. 41) noted that basal bone is cellular in “nearly all lower actinopterygian scales”.

Comparison. Many late Silurian–Early Devonian taxa have been resolved as stem osteichthyans, or basal actinopterygians, or basal sarcopterygians, but with little consensus about their relationships; *Ligulalepis* and *Meemannia* are the only taxa which have been recovered in all three positions in various cladistic analyses. The work by Lu *et al*. (2016, fig. 1F) elucidating the relationships of *Meemannia* indicated its dermal bones had a histological structure with a single layered enamel covering a dentine layer, pore openings on the dermal bone surface, leading into a canal network in the base of the ornament layer. Lu *et al*. (2016, p. 1) noted that “*Meemannia* presents an intriguing mosaic of characters: histology interpreted as a precursor to the ‘‘cosmine’’ of rhipidistian sarcopterygians (lungfishes plus tetrapods) combined with an undivided braincase and skull roof resembling that of actinopterygians”. However, the canal networks in actinopterygians (also *Andreolepis*, *e.g.*, Qu *et al*., 2017, fig. 4, and *Ligulalepis*, see Schultze, 1968, fig. 4) differ from the pore canal network of sarcopterygians. In actinopterygians, *Andreolepis*, and *Ligulalepis*, the pores between ornament tubercles and ridges on dermal bone and scales open to canals running into the horizontal vascular canal network underlying the dentine; *Andreolepis* possibly also has rare pores leading to separate cavities (Qu *et al*., 2017). The surface of *Meemannia* dermal bone resembles that of basal sarcopterygians, with a flat surface pierced by more or less regularly arranged large pores (Zhu *et al*., 2010, fig. 3B), which were considered to lead into a pore canal network with flask-shaped pore cavities. Horizontal canals connecting adjacent pore cavities and also dentinal pulp cavities were both described as extending out from the pore cavities, rather than forming separate networks. Lu *et al*. (2016) considered that the pore distribution and canal network is very similar to that of actinopterygian *Cheirolepis trailli* and basal sarcopterygian *Psarolepis romeri* (Lu *et al*., 2016, fig. 3). *Ligulalepis* differs from these taxa in having a histological structure of dermal bone (Fig. 6G–6J) and scales (Schultze, 1968, fig. 5) more similar to that of actinopterygians lacking superposed enamel/ganoine layers, such as *Moythomasia* (Jessen, 1968, fig. 6; Gardiner, 1984, fig. 143; Schultze, 2016, fig. 5).

Of the other basal osteichthyans, *Sparalepis tingi* shows a similar density of pores on dermal bones as in *Meemannia*, but has ornament ridges on scales and some dermal bones (Choo *et al*., 2017, figs. 3, 5). *Guiyu oneiros* (Zhu *et al*., 2009, fig. 4) has more distinct ornament ridges, presumably with small pore openings at their bases that are not visible in published images. Unfortunately, histological structure is unknown for both *Sparalepis* and *Guiyu*. In basal sarcopterygian *Psarolepis romeri*, separate pore canal and vascular canal networks are developed (*e.g.*, Qu *et al*., 2017, figs. 5, 9), with an organisation viewed as transitional to the cosmine structure of more derived sarcopterygians. In actinopterygians and *Ligulalepis*, however, the surface is covered with ridges and tubercles bearing distinctive oblique microridges, with a seemingly irregular arrangement of pores of vascular canals opening out between the ornament ridges. Sometimes the canals extended up through the ornament, presumably when the ridges and tubercles grew round them (*e.g.*, Fig. 5A, 5B).

Phylogenetic analysis

As noted earlier, recent cladistic analyses of early vertebrate relationships (*e.g.*, Lu *et al*., 2017, fig. 3; Clement *et al*., 2018, fig. 10A) have shown ’*Ligulalepis*’ as a stem osteichthyan, although King *et al*. (2017, fig. 3) and Zhu *et al*. (2021, fig. S4A) recovered the taxon

as a stem actinopterygian in BEAST2 and strict consensus trees respectively. Based on the new material described here, and previously described scales, we have added codings of scale and post-cranial characters for *Ligulalepis* (Supplementary Information), and reanalysed the character matrix of Clement *et al*. (2018), which is based on that of Lu *et al*. (2017). Two additional characters 45 and 156 were added. Our TNT parsimony analysis recovered 169 trees with a length of 808 steps; CI 0.369 RI 0.792. The strict consensus tree (Fig. 8) is identical to that of Clement *et al*. (2018, fig. 10A); examples of other trees are given in the supplementary figure. Thus even with the new post-cranial morphological and histological data, our strict consensus result still supports *Ligulalepis* as a basal osteichthyan, crownward to *Dialipina*, as the sister group to all other osteichthyans. This position concurs with the conclusions of Friedman and Brazeau (2010), who listed the osteichthyan synapomorphies found in *Ligulalepis*: rhombic scales with peg-and-socket articulation; enamel; large dermal bones contributing to skull roof; endochondral bone; ethmoid and sphenoid regions of neurocranium co-mineralized, with probable perichondral enclosure of nasal capsules. Those authors also noted that *Ligulalepis* lacks both actinopterygian and sarcopterygian synapomorphies.

DISCUSSION AND CONCLUSIONS

The discovery of new material for *Ligulalepis* adds to our knowledge of basal osteichthyan morphology. Several of the new *Ligulalepis* elements described here show unexpected features. The most notable example is the jaw element apparently comprising a composite jugal and maxillary bone. The only Palaeozoic fish known to have a comparable dermal element extending between the postero-ventral edge of the orbit and the lower margin of the upper jaw are coelacanths, with their adentate jugals.

Other interesting elements are the spine fragments. Certainly, no actinopterygians are known that have spines of this type, forming tapering cylinders ornamented all round with longitudinal enamel-topped ridges. The closest structures we can identify are the spines on the median dorsal plate and cleithrum in stem osteichthyan *Sparalepis* (Choo *et al*., 2017, fig. 2A). Scales comprising the squamation of *Sparalepis* look similar to the isolated scales of '*Ligulalepis*' *yunnanensis* Wang & Dong, 1989 found in the Ludlow Miaokao and Kuanti formations, overlying the Yuejiashan Formation from which *Guiyu* and *Sparalepis* were recovered. Scales of both *Sparalepis* and *'Ligulalepis*' *yunnanensis* share many features with those of *L. toombsi*. As well as being similarly proportioned in length and width to *Ligulalepis* flank scales, *Sparalepis tingi* scales have a prominent anterodorsal process (Choo *et al*., 2017, fig. 6C, labelled as the peg) like the diagnostic tongue-like one on the *Ligulalepis toombsi* holotype scale (Schultze, 1968, p. 345, fig. 1a, 1b), and both *Sparalepis* and '*L*.' *yunnanensis* have primary and secondary keels on the inner surface of the scale base (Choo *et al*., 2017, fig. 6A–6D), also like those deemed diagnostic for *Ligulalepis* (Schultze, 1968, p. 345, figs. 1b, 3b). By our assessment, the *Sparalepis* posterior flank squamation and scales figured by Choo *et al*. (2017, fig. 6) lack a peg, but typically mid and posterior flank scales on actinopterygians (also inferred for *L. toombsi*, Burrow, 1994) lack or have a reduced peg (*e.g*., Esin, 1990). If *Sparalepis* scales originally had more prominent posterior denticulations on the ornament ridges (possibly obscured/removed by manual preparation of the specimens), their morphology would compare very closely with those of '*L*.' *yunnanensis*, as far as can be seen from surface examination, differing mainly in the latter showing overlapping/overgrowth of ornament ridges. Indeed, Schultze *et al*. (2021) assigned this species to *Sparalepis*. Histological structure of *Sparalepis tingi* scales has not yet been described.

Our reassessment of the histological structure of *Ligulalepis* teeth, indicating that an acrodin cap is not present in any of the thin sections examined, resolves the anomaly caused by the recent mis-identification of an acrodin cap (Schultze, 2016), a feature deemed diagnostic for actinopterygians more crownward than *Cheirolepis*. Some features of *Ligulalepis* –in particular, the scale and dermal bone ornament morphology and histology– are more actinopterygian-like than in *Meemannia*, which resolves as more highly derived in most phylogenetic analyses. However, the cranial characters for *Ligulalepis* apparently outweigh the histological and postcranial characters, and our phylogenetic analysis reiterates its position as a stem osteichthyan (Fig. 8; Supplementary Fig.).

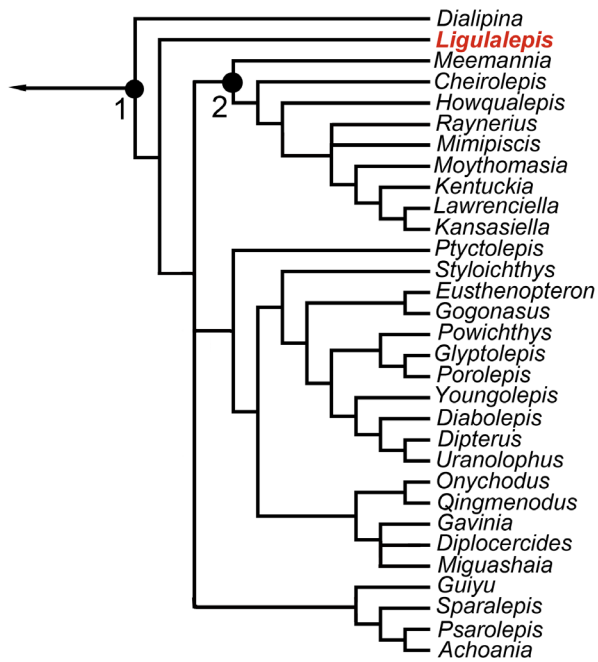

Figure 8. The osteichthyan branch of the strict consensus tree of 169 shortest length trees from our cladistic analysis: 1 is the osteichthyan node, 2 is the actinopterygian node.

Supplementary information. Supplementary material for this manuscript is available at the Spanish Journal of Palaeontology web-site (https://sepaleontologia.es/spanish-journal-palaeontology/) linked to this contribution. Mesquite file Burrow_Ligulalepis.nex and text file Burrow-ligulalepis textdata give the nexus matrix for the phylogenetic analysis, character list and changed codings list are given in Burrow_char_list.doc. The supplementary figure is denoted Burrow_suppl_fig.pdf. CT data for the 3D scans used in this study is available on Figshare (https://figshare.com/account/articles/22696975).

Supplementary Figure. Phylogenetic trees generated from our cladistic analysis: stem and osteichthyan taxa displayed, with stem and crown group chondrichthyans omitted. **A,** Strict consensus of 169 shortest length trees; **B,** bootstrap analysis; **C,** strict consensus tree showing synapomorphies common to 169 shortest length trees.

Author contributions. CB conceived the study, CB, JL, and GY analysed the data, and wrote the manuscript.

Competing Interest. We declare no competing interests

Funding. JL was supported by the Strategic Priority Research Program of Chinese Academy of Sciences (XDB26000000), National Science Fund for Excellent Young Scholars (42022011), and the National Natural Science Foundation of China (41872023).

Author details. **Carole J. Burrow**[1], **Gavin C. Young**[2] & **Jing Lu**[3]. [1]Geosciences Programme, Queensland Museum, 122 Gerler Rd, Hendra Qld 4011, Australia, carole.burrow@gmail.com; [2]Department of Applied Mathematics, Research School of Physics and Engineering, Australian National University ACT 2601, Australia, gavinyoung51@gmail.com; [3]Key Laboratory of Vertebrate Evolution and Human Origins of Chinese Academy of Sciences, Institute of Vertebrate Paleontology and Paleoanthropology, Chinese Academy of Sciences, Beijing 100044, China, lujing@ivpp.ac.cn.

Acknowledgements. We would like to acknowledge the debt we all owe to Tiiu Märss and Philippe Janvier for their work on Silurian stem osteichthyans, in particular *Andreolepis* and *Lophosteus*, as well as on all those jawless fishes. We thank Zerina Johanson (NHMUK) for access to specimens, and editors Carlos Martínez Pérez and Héctor Botella, reviewer Brian Choo, and an anonymous reviewer for their valuable input. CJB acknowledges the support (nonfinancial) of the Queensland Museum, and we acknowledge the Willi Hennig Society for the free distribution of TNT. This work is a contribution to the Special Volume dedicated to Dr Philippe Janvier and Dr Tiiu Märss.

REFERENCES

Agassiz, L. (1835). *Recherches sur les Poissons fossiles,* vol. II, part I, pp. 128–134 (1835), Plates 1D and 1E (1836). Neuchâtel.

Arratia, G., & Cloutier, R. (1996). Reassessment of the morphology of *Cheirolepis canadensis* (Actinopterygii). In H.-P. Schultze, & R. Cloutier (Eds.), *Devonian fishes and plants of Miguasha, Quebec, Canada* (pp. 165–197). Verlag Dr Friedrich Pfeil.

Basden, A. (2001). Early Devonian fish faunas of eastern Australia documentation and correlation. (PhD thesis, Macquarie University, Sydney).

Basden, A. M., & Young, G. C. (2001). A primitive actinopterygian neurocranium from the Early Devonian of southeastern Australia. *Journal of Vertebrate Paleontology*, *21*, 754–766.

Basden, A. M., Young, G. C., Coates, M. I., & Ritchie, A. (2000). The most primitive osteichthyan braincase? *Nature*, *403*, 185–188. doi:10.1038/35003183

Brazeau, M. D. (2009). The braincase and jaws of a Devonian 'acanthodian' and modern gnathostome origins. *Nature*, *457*, 305–308. doi: 10.1038/nature07436

Burrow, C. J. (1994). Form and function in scales of *Ligulalepis toombsi* Schultze, a palaeoniscoid from the Early Devonian of Australia. *Records of the South Australian Museum*, *27*, 175–185.

Burrow, C., Blaauwen, J. den, Newman, M., & Davidson, R. (2016). The diplacanthid fishes (Acanthodii, Diplacanthiformes, Diplacanthidae) from the Middle Devonian of Scotland. *Palaeontologia Electronica*, *19.1.10A*, 1–83. doi: 10.26879/601

Burrow, C. J., Davidson, R. G., den Blaauwen, J. L., & Newman, M. J. (2015). Revision of *Climatius reticulatus* Agassiz, 1844 (Acanthodii, Climatiidae), from the Lower Devonian of Scotland, based on new histological and morphological data. *Journal of Vertebrate Paleontology*, *35*(3), e913421. doi: 10.1080/02724634.2014.913421

Burrow, C. J., Newman, M., Blaauwen, J. D., Jones, R., & Davidson, R. (2018). The Early Devonian ischnacanthiform acanthodian *Ischnacanthus gracilis* (Egerton, 1861) from the Midland Valley of Scotland. *Acta Geologica Polonica*, *68*(3), 335–362. doi: 10.1515/agp-2018-0008

Choo, B. (2011). Revision of the actinopterygian genus *Mimipiscis* (=*Mimia*) from the Upper Devonian Gogo Formation of Western Australia and the interrelationships of the early Actinopterygii. *Earth and Environmental Science Transactions of the Royal Society of Edinburgh*, *102*, 77–104. doi: 10.1017/S1755691011011029

Choo, B. (2015). A new species of the Devonian actinopterygian *Moythomasia* from Bergisch Gladbach, Germany, and fresh observations on *M. durgaringa* from the Gogo Formation of Western Australia. *Journal of Vertebrate Paleontology*, *35*(4), e952817. doi: 10.1080/02724634.2015.952817

Choo, B., Long, J. A., & Trinajstic, K. (2009). A new genus and species of basal actinopterygian fish from the Upper Devonian Gogo Formation of Western Australia. *Acta Zoologica*, *90*, 194–194. doi: 10.1111/j.1463-6395.2008.00370.x

Choo, B., Lu, J., Giles, S., Trinajstic, K., & Long, J. A. (2019). A new actinopterygian from the Late Devonian Gogo Formation, Western Australia. *Papers in Palaeontology*, *5*(2), 343–363. doi: 10.1002/spp2.1243

Choo, B., Zhu, M., Qu, Q., Yu, X., Jia, L., & Zhao, W. (2017). A new osteichthyan from the late Silurian of Yunnan, China. *PLoS ONE*, *12*, e0170929. doi: 10.1371/journal.pone.0170929

Clement, A. M., King, B., Giles, S., Choo, B., Ahlberg, P. E., Young, G. C., & Long, J. A. (2018). Neurocranial anatomy of an enigmatic Early Devonian fish sheds light on early osteichthyan evolution. *ELife*, *7*, e34349. doi: 10.7554/eLife.34349

Davis, S. P., Finarelli, J. A., & Coates, M. I. (2012). *Acanthodes* and shark-like conditions in the last common ancestor of modern gnathostomes. *Nature*, *486*, 247–250. doi: 10.1038/nature11080

Esin, D. (1990). The scale cover of *Amblypterina costata* (Eichwald) and the paleoniscid taxonomy based on isolated scales. *Paleontology Journal*, *2*, 90–98.

Friedman, M., & Brazeau, M. D. (2010). A reappraisal of the origin and basal radiation of the Osteichthyes. *Journal of Vertebrate Paleontology*, *30*(1), 36–56. doi: 10.1080/02724630903409071

Gardiner, B. G. (1984). The relationships of the palaeoniscid fishes, a review based on new specimens of *Mimia* and *Moythomasia* from the Upper Devonian of Western Australia. *Bulletin of The British Museum (Natural History) Geology*, *37*, 173–428.

Gardiner, B. G., & Bartram, A. W. H. (1977). The homologies of ventral cranial fissures in osteichthyans. In S. M. Andrews, R. S. Miles, & A. D. Walker (Eds.), *Problems in Vertebrate Evolution* (pp. 227–245). Academic Press.

Giles, S., Friedman, M., & Brazeau, M. D. (2015a). Osteichthyan-like cranial conditions in an Early Devonian stem gnathostome. *Nature*, *520*, 82–85. doi: 10.1038/nature14065

Giles, S., Darras, L., Clément, G., Blieck, A., & Friedman, M. (2015b). An exceptionally preserved Late Devonian actinopterygian provides a new model for primitive cranial anatomy in ray-finned fishes. *Proceedings of the Royal Society of London B: Biological Sciences*, *282*(1816), 20151485. doi: 10.1098/rspb.2015.1485

Goloboff, P. A., Farris, J. S., & Nixon, K. C. (2008). TNT: Tree analysis using New Technology. Vers. 1.5. http://www.lillo.org.ar/phylogeny/tnt/

Gross, W. (1968). Fragliche Actinopterygier-Schuppen aus dem Silur Gotlands. *Lethaia*, *1*, 184–218.

Gross, W. (1969). *Lophosteus superbus* Pander, ein Teleostome aus dem Silur Oesels. *Lethaia*, *2*, 15–47.

Janvier, P. (1978). On the oldest known teleostome fish *Andreolepis hedei* Gross (Ludlow of Gotland), and the systematic position of the lophosteids. *Eesti NSV teaduste Akadeemia Toimetised, Geoloogia*, *27*, 86–95.

Jerve, A., Qu, Q., Sánchez, S., Blom, H., & Ahlberg, P. E. (2016). Three-dimensional paleohistology of the scale and median fin spine of *Lophosteus superbus* (Pander, 1856). *PeerJ, 4*, e2521. doi: 10.7717/peerj.2521

Jessen, H. (1968). *Moythomasia nitida* Gross und *M.* cf. *striata* Gross, devonische Palaeonisciden aus dem Oberen Plattenkalk der Bergisch-Gladbach - Paffrather Mulde (Rheinisches Schiefergebirge). *Palaeontographica Abteilung A*, *128*(4–6), 87–114.

Jones, S. L., Fitzherbert, J. A., Waltenberg, K., & Bodorkos, S. (2020). New SHRIMP U-Pb zircon ages from the Cobar Basin, New South Wales: Mineral Systems Projects, July 2018-June 2019. Geoscience Australia, Canberra. doi: 10.11636/Record.2020.042

King, B., Qiao, T., Lee, M. S. Y., Zhu, M., & Long, J. A. (2017). Bayesian Morphological Clock Methods resurrect placoderm monophyly and reveal rapid early evolution in jawed vertebrates. *Systematic Biology*, *66*(4), 499–516. doi: 10.1093/sysbio/syw107

Long, J. A. (1988). New palaeoniscoid fishes from the Late Devonian – Early Carboniferous of Victoria, Australia. *Memoirs of the Association of Australasian Palaeontologists*, *7*, 1–64.

Long, J. A., Mark-Kurik, E., Johanson, Z., Lee, M. S. Y., Young, G. C., Min, Z., Ahlberg, P. E., Newman, M., Jones, R., Blaauwen, J. den, Choo, B., & Trinajstic, K. (2015). Copulation in antiarch placoderms and the origin of gnathostome internal fertilization. *Nature*, *517*, 196–199. doi: 10.1038/nature13825

Lu, J., Giles, S., Friedman, M., den Blaauwen, J. L., & Zhu, M. (2016). The oldest actinopterygian highlights the cryptic early history of the hyperdiverse ray-finned fishes. *Current Biology*, *26*(12), 1602–1608. doi: 10.1016/j.cub.2016.04.045

Lu, J., Giles, S., Friedman, M., & Zhu, M. (2017). A new stem sarcopterygian illuminates patterns of character evolution in early bony fishes. *Nature Communications*, *8*(1), 1932. doi: 10.1038/s41467-017-01801-z

Lund, R., & Lund, W. L. (1985). Coelacanths from the Bear Gulch Limestone (Namurian) of Montana and the evolution of the Coelacanthiformes. *Bulletin of the Carnegie Museum of Natural History*, *25*, 1–74.

Lund, R., & Poplin, C. (1997). The rhadinichthyids (paleoniscoid actinopterygians) from the Bear Gulch Limestone of Montana (USA, Lower Carboniferous). *Journal of Vertebrate Paleontology, 17*(3), 466–486. doi:10.1080/02724634.1997.10010996

Pander, C. H. (1856). *Monographie der fossilen Fische des silurischen Systems der Russisch-Baltischen Gouvernements. Obersilurische Fische*. Buchdruckerei der Kaiserlichen Akademie der Wissenschaften.

Pearson, D. M., & Westoll, T. S. (1979). The Devonian actinopterygian *Cheirolepis* Agassiz. *Transactions of the Royal Society of Edinburgh. Earth Sciences*, *70*, 337–399.

Qu, Q., Sánchez, S., Zhu, M., Blom, H., & Ahlberg, P. E. (2017). The origin of novel features by changes in developmental mechanisms: ontogeny and three-dimensional microanatomy of polyodontode scales of two early osteichthyans. *Biological Reviews*, *92*, 1189–1212. doi: 10.1111/brv.12277

Schultze, H.-P. (1968). Palaeoniscoidea-Schuppen aus dem Unterdevon Australiens und Kanadas und aus dem Mitteldevon Spitsbergens. *Bulletin of the British Museum of Natural History (Geology)*, *16*, 343–368.

Schultze, H.-P. (1992). Early Devonian actinopterygians (Osteichthyes, Pisces) from Siberia. In E. Mark-Kurik (Ed.), *Fossil Fishes as Living Animals*. *Academia*, *1*, 233–242.

Schultze, H.-P. (2016). Scales, enamel, cosmine, ganoine, and early osteichthyans. *Comptes Rendus Palevol*, *15*, 83–102. doi: 10.1016/j.crpv.2015.04.001

Schultze, H.-P., & Cumbaa, S. L. (2001). *Dialipina* and the characters of basal actinopterygians. In P. E. Ahlberg (Ed.), *Major Events in Early Vertebrate Evolution: Palaeontology, Phylogeny, Genetics and Development* (pp. 316–332). Taylor & Francis.

Schultze, H.-P., Mickle, K. E., Poplin, C., Hilton, E. J., & Grande, L. (2021). *Handbook of Paleoichthyology. Vol. 8A. Actinopterygii I. Palaeoniscimorpha, Stem Neopterygii, Chondrostei*. Verlag Dr Friedrich Pfeil.

Sherwin, L. (1996). Narromine 1:250000 Geological Sheet SI/55-3: Explanatory notes. Geological Survey of New South Wales.

Wang, N.-Z., & Dong, Z.-Z. (1989). Discovery of Late Silurian microfossils of Agnatha and fishes from Yunnan, China. *Acta Palaeontologica Sinica*, *28*(2), 192–206.

Whiteaves, J. (1881). On some fossil fishes, Crustacea, and Mollusca from the Devonian rocks at Campbelltown, N. B., with descriptions of five new species. *Canadian Naturalist and Geologist*, *10*, 93–101.

Yu, X. (1998). A new porolepiform-like fish, *Psarolepis romeri*, gen. et sp. nov. (Sarcopterygii, Osteichthyes) from the Lower Devonian of Yunnan, China. *Journal of Vertebrate Paleontology*, *18*(2), 261–274.

Zhu, M., & Schultze, H.-P. (1997). The oldest sarcopterygian fish. *Lethaia*, *30*(4), 293–304. doi: 10.1111/j.1502-3931.1997.tb00472.x

Zhu, M., Wang, W., & Yu, X. (2010). *Meemannia eos*, a basal sarcopterygian fish from the Lower Devonian of China – expanded description and significance. In D. K. Elliott, J. G. Maisey, X. Yu, & D. Miao (Eds.), *Morphology, Phylogeny and Paleobiogeography of Fossil Fishes* (pp. 199–214). Verlag Dr. Friedrich Pfeil.

Zhu, M., Yu, X., & Janvier, P. (1999). A primitive fossil fish sheds light on the origin of bony fishes. *Nature*, *397*, 607–610. doi: 10.1038/17594

Zhu, M., Yu, X., Wang, W., Zhao, W., & Jia, L. (2006). A primitive fish provides key characters bearing on deep osteichthyan phylogeny. *Nature*, *441*, 77–80. doi: 10.1038/nature04563

Zhu, M., Zhao, W., Jia, L., Lu, J., Qiao, T., & Qu, Q. (2009). The oldest articulated osteichthyan reveals mosaic gnathostome characters. *Nature*, *458*, 469–474. doi: 10.1038/nature07855

Zhu, M., Yu, X., Ahlberg, P. E., Choo, B., Lu, J., Qiao, T., Qu, Q., Zhao, W., Jia, L., Blom, H., & Zhu, Y.-A. (2013). A Silurian placoderm with osteichthyan-like marginal jaw bones. *Nature*, *502*, 188–193. doi: 10.1038/nature12617

Zhu, Y.-A., Giles, S., Young, G. C., Hu, Y., Bazzi, M., Ahlberg, P. E., Zhu, M., & Lu, J. (2021). Endocast and bony labyrinth of a Devonian "placoderm" challenges stem gnathostome phylogeny. *Current Biology*, *31*(5), 1112–1118, e4. doi: 10.1016/j.cub.2020.12.046

Zylberberg, L., Meunier, F. J., & Laurin, M. (2015). A microanatomical and histological study of the postcranial dermal skeleton of the Devonian actinopterygian *Cheirolepis canadensis*. *Acta Palaeontologica Polonica*, *61*, 363–376. doi: 10.4202/app.00161.2015